Catalysis Today 181 (2012) 108–115

Contents lists available at ScienceDirect

Catalysis Today

journal homepage: www.elsevier.com/locate/cattod

On the role of lattice/surface oxygen in ceria–zirconia catalysts for diesel soot combustion

Eleonora Aneggi, Carla de Leitenburg, Alessandro Trovarelli*

Dipartimento di Chimica, Fisica e Ambiente, Università di Udine, via Cotonificio 108, 33100 Udine, Italy

ARTICLE INFO

Article history:
Received 28 February 2011
Received in revised form 12 May 2011
Accepted 27 May 2011
Available online 25 June 2011

Keywords:
Ceria
Ceria–zirconia
Soot oxidation
Diesel pollution control
Oxygen storage capacity
Combustion

ABSTRACT

A series of ceria and ceria–zirconia catalysts with varying composition and surface area have been systematically investigated in the oxidation of soot in the range of temperature 600 K < *T* < 800 K. The samples have been characterized by their textural and structural properties and formation of homogeneous solid solutions has been confirmed. The activity in soot combustion has been measured both in the presence and absence of gas-phase O_2 in order to characterize the contribution of surface and bulk properties of the materials. It was shown that the number of active surface oxygen linked to ceria plays a major role, while oxygen storage capacity, governed by introduction of zirconia, can be important when and where oxidation of soot particles is operated in the absence or defect of gaseous oxygen. The role of Zr in stabilizing surface area of ceria (thus increasing the number of surface active sites) is also important when evaluating the effect of composition on soot oxidation activity.

1. Introduction

In the last years, the attention on negative effects of particulate matter generated from diesel engines has rapidly grown and as a consequence the regulations on emissions become more stringent. The legislative emission standards for diesel engine vehicles suggest that, beside the results obtained by improving the engine technology and the fuel quality, the employment of treatment systems able to enforce the standards on soot emissions will be necessary. As a consequence, various emission-reduction technologies have been developed and among them, filtering followed by catalytic oxidation is particularly interesting [1,2]. A major issue associated with this approach is the difficulty of spontaneous filter regeneration during soot combustion. Several catalyst formulations have been studied for this purpose with the aim of reducing combustion temperature of soot below 600 K [3–17]. The use of NO/O_2 mixtures as oxidizing agent to shift the onset of oxidation at lower temperatures was also extensively employed in the last years [11,18–23].

Regarding the intimate mechanism involved in the oxidation of carbon under O_2 atmosphere, several authors pointed out the importance of redox properties of the catalyst. That is, the effectiveness of the catalyst can be related to its ability to deliver oxygen from the lattice to the gas phase (or better to the solid carbon reactant) in a wide temperature range [7]. Recently, it has been reported that the use of catalyst formulations based on cerium oxide or CeO_2 doped with transition metals [8,11,24–26], rare earth elements [27,28,30–34] or alkali metals [8,11,29,35,36] confers interesting properties to soot combustion catalysts due to high availability of surface oxygen and high surface reducibility. The success of oxygen storage systems based on ceria is due to their ability to change oxidation state during operation (i.e. CeO_2 to CeO_{2-x}) maintaining structural integrity, thus allowing oxygen uptake and release to occur easily. In addition to the redox features many other factors can help improving the ability of ceria in soot oxidation. For example the key role of ceria–soot interface region and therefore of the ceria–soot contact has been demonstrated to be strongly involved in the dynamic of reaction promoting the rate of transfer of oxygen at much lower temperatures [13,37,38]. Doping of ceria with other rare earth or transition elements further promotes surface oxygen availability for oxidation reaction thus contributing to lower oxidation temperatures. A very well known dopant for ceria is zirconium, which promotes bulk oxygen mobility in ceria–zirconia solid solutions [39]. State of the art material for oxygen storage in three-way catalysts (TWC) is constituted by ceria and ceria–zirconia eventually doped with small amounts of rare earth elements, added to enhance the redox features of ceria [40]. In this case homogeneity of solid solutions, structural features and composition are the key parameters in successful catalyst design. Since it is reported in the literature that strong relationships exist

* Corresponding author. Tel.: +39 0432558855; fax: +39 0432558803.
E-mail address: trovarelli@uniud.it (A. Trovarelli).

0920-5861/$ – see front matter © 2011 Elsevier B.V. All rights reserved.
doi:10.1016/j.cattod.2011.05.034

between oxygen storage/redox capacity and soot combustion activity [25,27,41,42], it is of interest to investigate if the knowledge that has been accumulated on redox systems for TWC can help in developing more active soot combustion catalysts. Although ceria–zirconia based materials have been studied as catalyst for soot combustion [14,16,25–27,31–34], there are many parameters that can heavily affect their functioning under reaction conditions and a unifying picture is still missing. In several studies the key role of surface area/composition and oxygen storage capacity was taken into account but, so far, their relative importance has not been investigated in detail especially under conditions of varying gas-phase oxygen concentration. The purpose of this work is to gain further insights into the influence of surface area and OSC in soot combustion over ceria–zirconia catalysts and evaluate the parameters that govern the activity.

2. Materials and methods

2.1. Catalyst preparation and characterization

Ceria–zirconia solid solutions, in the entire composition range, were prepared by coprecipitation at pH 9.5 starting from nitrates in the presence of H_2O_2 (a key parameter to increase the surface area and the OSC of the materials) and using ammonia as precipitating agent [43] Precipitates were dried at 393 K and calcined at different temperatures from 773 (fresh materials) to 1273 K, for 3 h. They will be indicated as CZXX-T, where XX is the Ce/(Ce + Zr) atomic ratio (% unit) and T the temperature of calcination.

Textural characteristics of all fresh samples were measured according to the B.E.T. method by nitrogen adsorption at 77 K, using a Tristar 3000 gas adsorption analyzer (Micromeritics).

Structural features of the catalysts were characterized by X-ray diffraction (XRD). XRD patterns were recorded on a Philips X'Pert diffractometer operated at 40 kV and 40 mA using nickel-filtered Cu-K_α radiation. Spectra were collected using a step size of 0.02° and a counting time of 40 s per angular abscissa in the range 20–145°. The Philips X'Pert HighScore software was used for phase identification. The mean crystalline size was estimated from the full width at the half maximum (FWHM) of the X-ray diffraction peak using the Scherrer equation [44] with a correction for instrument line broadening. Rietveld refinement [45] of XRD pattern was performed by means of GSAS-EXPGUI program [46,47].

2.2. Reactivity measurements

The preparation of samples for catalytic measurements was carried out by grinding and mixing known amounts of soot and ceria–zirconia in a mortar for 10 min in order to obtain a tight contact [48]. The kind of contact between catalyst and soot is extremely important [7,49]: the tight contact conditions are poorly representative of the real working conditions experienced by the catalyst deposited in a catalytic trap, but they allow a rapid screen of catalysts under reproducible experimental conditions. Soot oxidation activity was tested by running TGA experiments (Q500, TA Instruments) either in the presence or in the absence of oxygen (N_2 atmosphere) [9,50–57]. Under oxygen a soot/catalyst weight ratio of 1:20 was adopted. The sample (soot + catalyst, ca. 20 mg) was placed in a small flat Pt crucible licked by an air flow (60 ml/min) tangent to the sample. As a measure of activity we used the temperature at which 50% of weight loss is observed (T50, corresponding to removal of 50% of soot). Reproducibility of results was tested by running several TG experiments on similar samples and the results in terms of T50 were always within ±3 K. A typical oxidation profile is shown in Fig. 1A (solid line).

To study the effect of lattice oxygen of ceria, soot oxidation activity experiments in the absence of gas phase oxygen were carried out in the same TG apparatus. The experiments consisted in a temperature programmed reduction under inert gas flow using known amounts of catalysts mixed with soot which acts as reductant. Samples were pre-treated for 1 h at 423 K to eliminate adsorbed water, and then they were heated under inert atmosphere (N_2@100 ml/min) at a constant rate (10 K/min) up to 1073 K. The weight loss of the sample is due to formation of CO/CO_2 and is a measure of activity of soot oxidation by oxygen from the catalyst. As a measure of activity we used the weight loss in the range from 423 to 1073 K. Fig. 1A (dotted line) depicts a representative profile showing loss of weight due to reaction between lattice oxygen and carbon particles.

Oxygen storage capacity (OSC) of samples was investigated by carrying out TGA experiments in Ar/(5%)H_2 mixture flow (100 ml/min). Each sample was treated in N_2 atmosphere for 1 h at 553 K, followed by heating at a constant rate (10 K/min) up to 673 K and kept at this temperature for 15 min, to eliminate the adsorbed water. Finally Ar/H_2 mixture was introduced while keeping the temperature at 673 K for 30 min. The observed weight loss (Fig. 1B) is due to oxygen removal by H_2 to form water, and it can

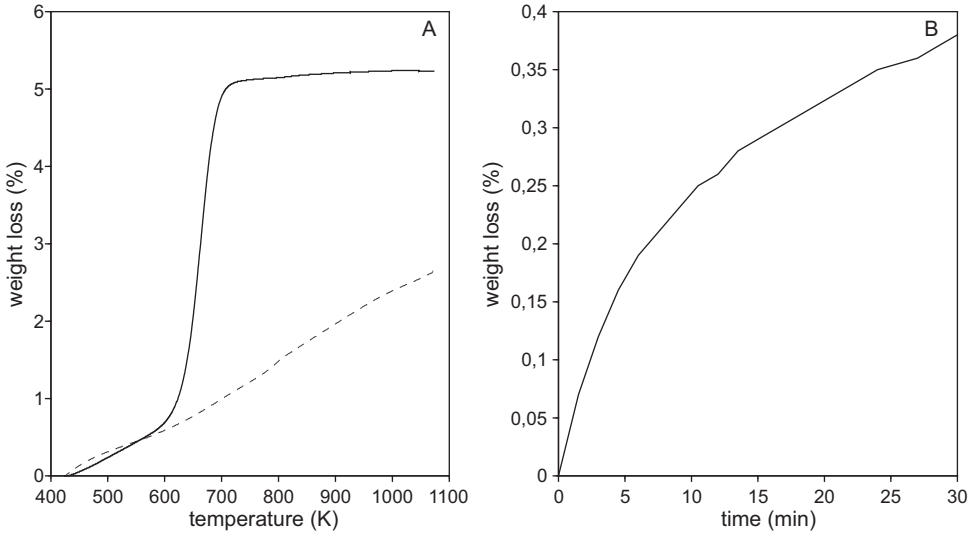

Fig. 1. (A) Weight loss profile measured in a typical experiment under air flow (solid line) and under inert atmosphere (dotted line); (B) weight loss due to reduction operated under Ar/H_2 mixtures in a typical OSC measurement.

Table 1
Textural and structural characterization of ceria and ceria–zirconia samples.

Sample	SA (m^2/g)	APoS[a] (nm)	PS (nm)[b]	Phase	Cell parameters Rietveld refinement		
					$a = b = c$ (Å)	$a' = b'$ (Å)	c (Å)
CZ100-773	53	15	12	Cubic	5.410 (1)		
CZ100-873	44	14	15	Cubic	5.410 (1)		
CZ100-973	35	18	18	Cubic	5.410 (1)		
CZ100-1073	26	18	23	Cubic	5.410 (1)		
CZ100-1173	17	21	32	Cubic	5.410 (1)		
CZ100-1273	6	17	50	Cubic	5.410 (1)		
CZ75-773	73	13	6	Cubic	5.368 (1)		
CZ75-873	58	14	7	Cubic	5.368(1)		
CZ75-973	49	17	8	Cubic	5.369(1)		
CZ75-1073	36	19	10	Cubic	5.370(1)		
CZ75-1173	24	25	14	Cubic	5.372(1)		
CZ75-1273	10	30	22	Cubic	5.369(1)		
CZ44-773	90	9	4	Tetragonal t′		3.707(1)	5.366(1)
CZ44-873	69	11	5	Tetragonal t′		3.709(1)	5.361(1)
CZ44-973	53	13	6	Tetragonal t′		3.713(1)	5.358(1)
CZ44-1073	33	18	7	Tetragonal t′		3.715(1)	5.355(1)
CZ44-1173	24	24	9	Tetragonal t′		3.716(1)	5.368(1)
CZ44-1273	12	28	7	Tetragonal t′ (50%)		3.691(1)	5.315(1)
				Tetragonal t′ (50%)		3.777(1)	5.389(1)
CZ28-773	90	7	7	Tetragonal t′		3.655(1)	5.267(1)
CZ28-873	75	8	7	Tetragonal t′		3.656(1)	5.266(1)
CZ28-973	59	9	8	Tetragonal t′		3.658(1)	5.267(1)
CZ28-1073	35	12	9	Tetragonal t′		3.658(1)	5.263(1)
CZ28-1173	26	16	11	Tetragonal t′		3.656(1)	5.259(1)
CZ28-1273	9	26	17	Tetragonal t′ (85%)		3.650(1)	5.249(1)
				Tetragonal t′ (15%)		3.728(1)	5.374(2)

[a] Average pore size.
[b] Particle size calculated by Scherrer equation [41].

be associated to total oxygen storage capacity at that temperature [26,58].

3. Results and discussion

3.1. Textural and structural characterization

Textural and structural characterization of all samples investigated in this study is reported in Table 1. Fresh materials have surface area in the range 50–90 m^2/g. Increasing the temperature of calcination the surface area progressively decreases and the particle size increases, due to the sintering induced by thermal treatment; the aging strongly influences all samples, with a more pronounced effect for Zr-free materials. In accordance with literature [59,60] the introduction of zirconia enhances the thermal stability of ceria-based systems and allows maintaining a greater surface area after aging which is an important issue in soot oxidation where the number of contact point between soot and catalyst is of primary importance.

The pore size distribution of each sample was evaluated from N_2 desorption isotherm. The isotherms for each sample are of type IV, typical of mesopouros materials. It is important to note that the first part of the isotherm is not very pronounced consequently materials do not present any microporosity as confirmed by the t-plot analysis. The intercept of the t-plot is almost zero for each sample and the surface area due to micropores is negligible. Moreover, the hysteresis is of type H3 (IUPAC classification) indicating a very wide pore size distribution. Fig. 2 shows that an increase in the amount of zirconia in the solid solution, induces changes in the pore size distribution with a shift to lower pore diameter (the trend is the same for each temperature of calcination and only materials calcined at 773 K are shown for sake of clarity).

The structural features of the samples analyzed by XRD are also shown in Table 1. All these materials form a solid solution between ceria and zirconia and XRD do not show any evident peak splitting due to the presence of mixed oxide phases. It is very well known that the method of synthesis and treatments strongly influenced structural characteristics of ceria–zirconia [61] and that transition to one structure to another may be critically influenced by several parameters [62]. Our measurements suggest that for binary ceria–zirconia samples with cerium content greater than 50 mol% the formation of a cubic fluorite lattice is favoured. This is in accordance with literature, where generally the limit for formation of a cubic (either cubic or tetragonal t′) solid solution is found at ca. 50 mol% CeO_2 [63]. Thus all our cerias

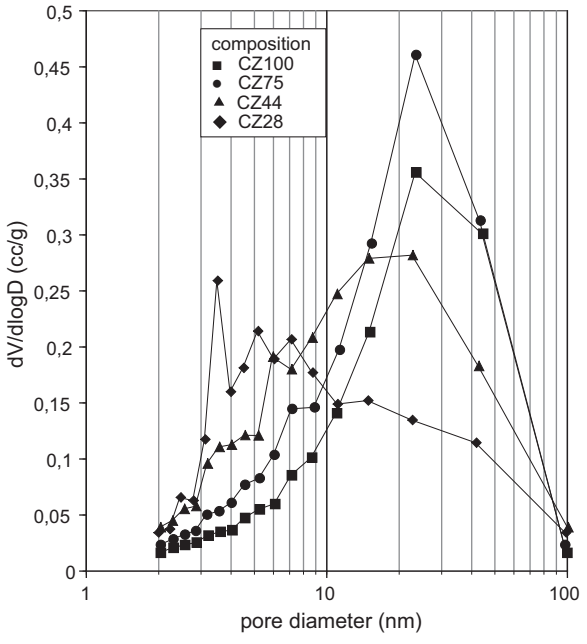

Fig. 2. Pore size distribution for samples calcined at 773 K (CZ100, ■; CZ75, ●; CZ44, ▲; CZ28, ♦).

crystallize in a cubic fluorite structure of *Fm*3*m* symmetry with almost identical cell parameters. A similar situation is found with CZ75 samples that crystallize in a cubic structure; the value of $a = 5.369$ fits well with data reported previously [62,64]. No indication of phase splitting is detected after aging, which is in line with what found on ceria-rich samples after similar treatments [65]. This however cannot exclude that thermal treatment might induce some phase assessment at a nano-scale level, with small compositional variations, which have been indicated as responsible for enhancement of oxygen exchange in samples obtained using similar procedures [58]. In the range of composition 25–45 mol% CeO_2 good agreement between the refinement and a tetragonal structural model confirms that all samples belong to the t′ tetragonal phase with space group $P4_2/nmc$. No peak splitting that would indicate the presence of two phases could be detected, and therefore, the diffraction patterns demonstrate the formation of a single solid solution-like ceria–zirconia phase (exception made for CZ44-1273 and CZ28-1273). Again, this cannot exclude the presence of different arrangements of oxygen sublattice or the presence of a multi-phase system at a nanoscale level, not detected by XRD. In both CZ44 and CZ28, after calcination at 1273 K, XRD features show a peak splitting that indicate a segregation into two t′ tetragonal phases with space group $P4_2/nmc$.

After calcinations, only a slight modification of the structural parameter is observed which does not affect overall phase distribution. In summary, XRD characterization of binary ceria–zirconia solid solutions confirms the homogeneity of samples (within the limits outlined above) with the identification of mainly cubic and tetragonal t′ phases [66].

3.2. Catalytic activity under O_2 atmosphere

CeO_2 as support/active catalyst in diesel soot oxidation has been the subject of several studies [3,8,10,11,30,67] aiming at finding a relationship between combustion activity under conditions typical of diesel exhaust and the characteristics of the materials. Some authors attribute a key role to the surface/textural properties of ceria [27,30,41] or to pore size distribution [68,69], others agree in explaining the activity of cerium oxide with its oxygen storage and redox capacity [14,24,70,71]. The introduction of Zr strongly modifies redox and structural/defect characteristics of pure ceria and the complexity of determining relations between activity and redox properties is further increased. One of the most important roles of CeO_2 in catalytic redox reactions is to provide surface active sites [72] and to act as an oxygen buffer providing oxygen storage/transport by shifting between Ce^{4+} and Ce^{3+} during reaction. That is, the presence of surface active oxygens from one side, and the oxygen storage capacity from the other, are among the most important factors to be considered. These, in turn, are strongly influenced by surface area and surface/bulk composition. In the following section we will try to correlate the variables mentioned above with soot oxidation activity both in the presence and absence of gas-phase oxygen in order to obtain a more general picture of the behaviour of these catalysts.

Fig. 3 shows the results of soot combustion studies carried out under air over ceria and ceria–zirconia. All the catalysts examined are active in promoting soot combustion in the range of temperature from ca. 600 K to 800 K. As a measure of activity the temperature at which 50% weight loss is observed (T50, corresponding to the temperature at which 50% of soot is converted under tight contact conditions) was used. These values are reported against composition for every calcination temperature and for each series the curve assumes an almost inverse volcano-type profile with a minimum in the middle composition range (CZ75). For ceria–zirconia, this is a typical characteristic of phenomena driven by the redox features of the catalyst [26,73].

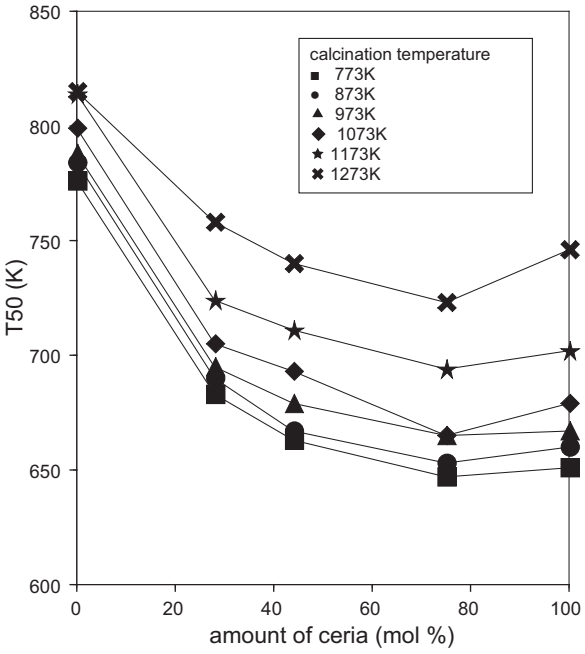

Fig. 3. T50 against composition as obtained from TG experiments over soot/catalyst mixtures under air.

Fig. 4 displays the activity against surface area for each composition. The activity shows a marked dependence against surface area; in particular a decrease in surface area leads to an increase in T50 in agreement with recent results [27,30,41]. Fig. 4 shows also that the behaviour of T50 is dependent on surface area values. For surface area above a value of ca. 40 m^2/g variation in T50 is less influenced by large variations of surface area while important effects in ΔT50 are observed for lower surface area values, as evidenced by a change in the slope of the curve at ca. 35-40 m^2/g. It is therefore important to maintain surface area above a minimum value to avoid a

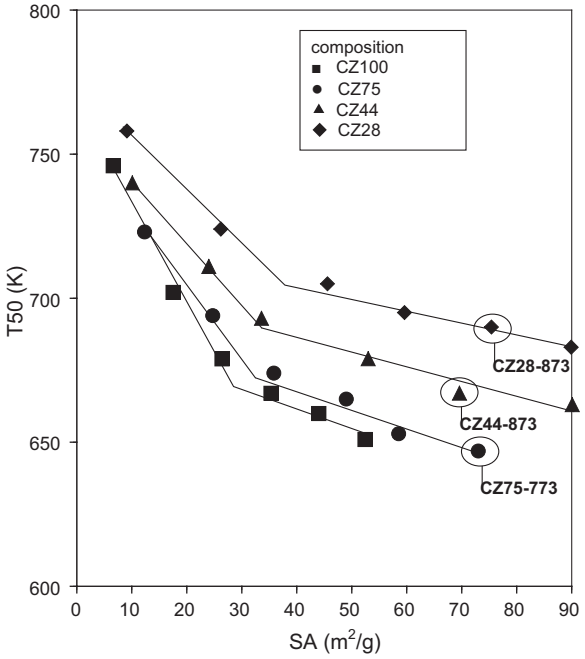

Fig. 4. T50 against surface area for each composition as obtained from TG experiments over soot/catalyst mixtures under air.

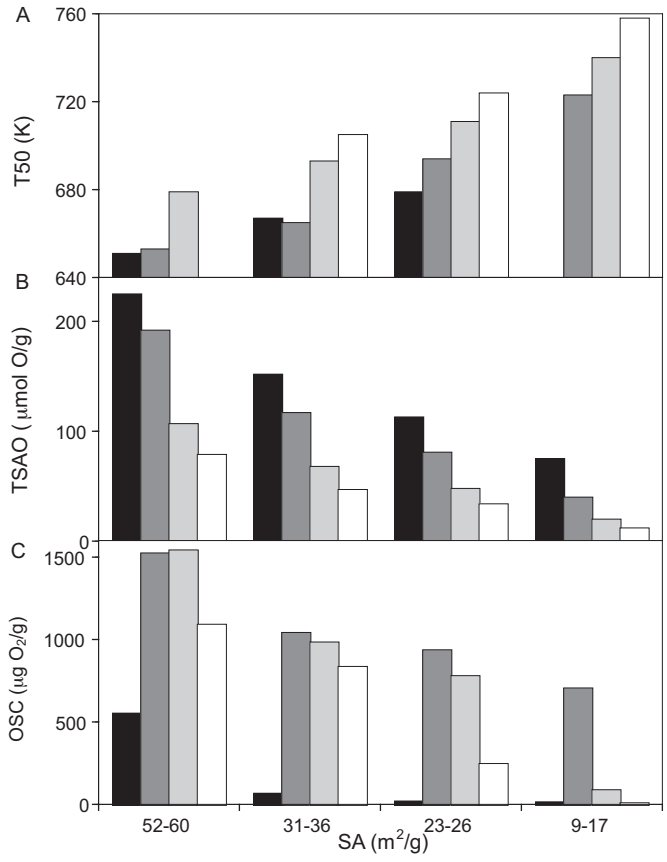

Fig. 5. (A) T50, (B) TSAO and (C) OSC for samples with different composition and similar surface area values: CZ100 (black), CZ75 (dark grey), CZ44 (light grey) and CZ28 (white).

large drop of activity. Fig. 4 also highlights that, catalyst formulations having similar surface area but different composition, show very different activity. For example, samples CZ75-773, CZ44-873 and CZ28-873 with surface area around 70 m^2/g (73, 69 and 75, respectively) shows very different T50 values (647 K, 667 K and 690 K, respectively). This is better evidenced in Fig. 5A where the values of T50 for samples with surface area values in the same range are reported, and samples with a higher amount of ceria result to be more active. While on average it is observed that activity increases by increasing surface area there are several samples which show similar values of T50 while having very different surface area. It seems therefore that surface area alone cannot explain the order of activity but this should take into account the right combination of surface area and composition. For that reason it is important to correlate overall activity with total available surface active oxygens (which are linearly dependent on the amount of ceria) and total oxygen storage capacity (which generally shows a volcano-type relation with composition, Table 2). The number of *total surface oxygens* (TSO) have been estimated according to Madier et al. [73] starting from the structure and the molar composition of the oxide considering the exposure of (1 0 0), (1 1 0) and (1 1 1) surfaces and assuming that Zr atoms do not participate to the redox process. The number of *total surface available oxygens* (TSAO) represents a fraction of total surface oxygens considering that only one atom out of four is involved in the Ce^{4+}–Ce^{3+} redox process [73–75]. OSC data were collected according to the method described in the experimental part. In agreement with data from the literature, OSC of homogeneous ceria–zirconia solid solutions is reported to be dependent on composition showing a maximum in the composition range $Ce_xZr_{1-x}O_2$ with $0.4 < x < 0.7$ [25,73,76]. Fig. 6(A and B) illustrates the relationships between activity and surface oxygens/OSC; there is a clear dependence of the activity against surface oxygens (Fig. 6A) with a large increase in T50 with decreasing available oxygens. Their number depends on surface area and composition; at constant surface area values, the number of surface oxygens is linearly dependent on the amount of ceria (Fig. 5B). Comparison between Fig. 5A and B shows that if samples with similar surface area are compared the catalysts with a higher amount of ceria and consequently a higher amount of available oxygens are more active. This is in line with what reported in literature, where the role of ceria is expected to be that of providing oxygen species to the soot at a temperature lower than that of the direct activation of gaseous O_2 by the carbon soot particles [37,38].

No clear correlation was found by comparing activity against OSC (Fig. 6B). Although as a weak indication oxidation temperature seems to decrease with OSC there are a few samples where large differences in OSC end up with the same T50. It is evident that the OSC of the catalyst does not have a predominant role in the reaction under lean atmosphere, where there is enough gas phase

Table 2
Total surface available oxygens and OSC.

Sample	OSC (μgO_2/g)	TSAO (μmol O/g)	Sample	OSC (μgO_2/g)	TSAO (μmol O/g)
CZ100-773	552	225	CZ44-773	2944	182
CZ100-873	345	189	CZ44-873	2074	141
CZ100-973	68	152	CZ44-973	1543	107
CZ100-1073	20	113	CZ44-1073	985	68
CZ100-1173	18	75	CZ44-1173	781	48
CZ100-1273	15	28	CZ44-1273	89	20
CZ75-773	1947	240	CZ28-773	1585	119
CZ75-873	1525	192	CZ28-873	1357	100
CZ75-973	1196	161	CZ28-973	1092	79
CZ75-1073	1043	117	CZ28-1073	837	47
CZ75-1173	937	81	CZ28-1173	248	34
CZ75-1273	706	40	CZ28-1273	10	12

Surface available oxygens are the estimate of surface O atoms available for reduction. The calculation was based on the assumption that all surface O associated with ceria is available for the redox reaction. Further we assume that O associated with Zr cannot be removed and that Zr is present on the surface in the same concentration as the bulk. Using these assumptions, the total surface available oxygens (TSAO) are calculated using the following equation:

$$\mathrm{TSAO} = \frac{SA(\mathrm{nm^2/g}) \cdot X_{Ce} \cdot O(\mathrm{atom/nm^2}) \cdot 10^6(\mathrm{mmol/mol}) \cdot 0.25}{N_A(\mathrm{atom/mol})}$$

where SA is the surface area, X_{Ce} the molar fraction of Ce in the material, N_A the Avogadro number and O is the number of total surface oxygens (TSO) calculated according to Ref. [73] considering the average exposure of (1 0 0)+(1 1 1)+(1 1 0) surfaces.

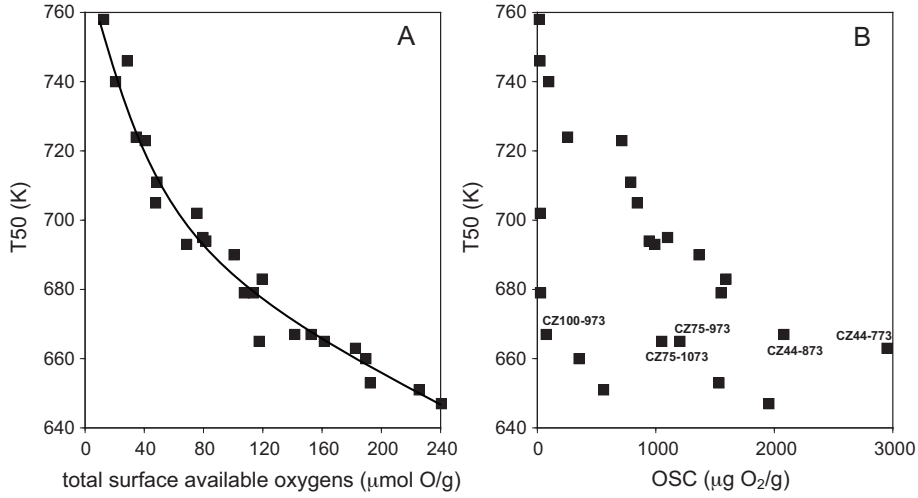

Fig. 6. T50 against total surface oxygen availability (A) and OSC (B) as obtained from TG experiments on soot/catalyst mixtures under air.

oxygen to refill surface oxygen sites when depleted by the reaction. The lack of correlation is also apparent from comparison of Fig. 5A and C where the effect of OSC is reported for samples with similar textural properties. It seems therefore by introduction of Zr does not have a direct beneficial effect on soot oxidation under air since it decrease the number of surface active oxidation site, which are directly dependent on the number of Ce atoms.

3.3. Catalytic activity under inert atmosphere

A rather different situation is found performing oxidation under an inert atmosphere. The TG profiles show a continuous weight loss starting at ca. 450 K with evolution of CO_2. In order to exclude contributions from O_2 desorption/removal from the sample, blank experiments on all catalysts were carried out by running a temperature programmed analysis in the absence of soot. The overall results are reported in Fig. 7 and as a measure of activity the weight loss was used. The curve has a maximum in the middle composition range, for each temperature of calcination, thus pointing out that participation of lattice oxygen in soot oxidation may contribute to overall activity. In Fig. 8 the dependence of activity against surface oxygens and OSC is shown. It is clearly seen that an almost linear relationship exists between oxidation activity and OSC while the data of activity against surface oxygens are rather scattered, although the overall behaviour evidences a slight positive effect. It is evident that in the absence of gaseous oxygen, when surface lattice oxygen of ceria–zirconia is utilized for soot oxidation the resultant vacant site is refilled by sub-surface/bulk oxygen and the dynamic of the process is governed by OSC of the catalyst. In this case the presence of Zr helps in creating structural defects which result in higher oxygen mobility.

A simple redox route mechanism for soot oxidation, which utilizes oxygen activated from the support in a typical reduction/oxidation path (Mars Van Krevelen type) in which the catalyst undergoes a partial reduction, can be envisaged. A schematic representation of soot oxidation arranged from that presented by Katta et al. [16] in the case of ceria–lanthana is reported in Fig. 9. In the presence of air the active surface oxygens spill/transfer over the soot leading to formation of CO/CO_2 which then desorbs in the gas phase; surface vacancy is readily replenished by gaseous O_2 with regeneration of surface active oxygen. In the absence of gaseous O_2 or in the case of oxidation of big soot particles where steric/geometric constrains prevent easy access of gas-phase oxygen the regeneration of surface oxygen is operated by sub-surface or bulk diffusion of lattice oxygen. It is therefore expected that nature, dimension, location of soot/catalyst interface will strongly affect this mechanism by changing the overall degree of participation of bulk oxygen to the soot oxidation mechanism. In a real situation both mechanism might coexist, with surface contributions prevailing over bulk lattice effects. This is well summarized by the different degree of spreading of the values of activity of the two curves of Fig. 6. The extent to which oxygen storage governs the overall activity under air cannot be clearly separated from other contributions but it is certainly important because it provides an alternative route for the oxidation of big soot particles in contact with ceria, where access of gas-phase oxygen is hindered by other factors.

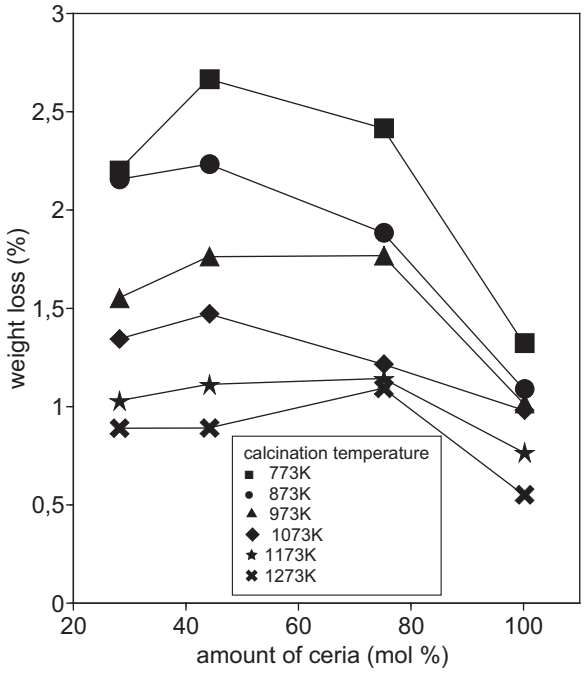

Fig. 7. Weight loss of ceria–zirconia samples subjected to temperature programmed reduction experiments in the presence of soot under inert atmosphere.

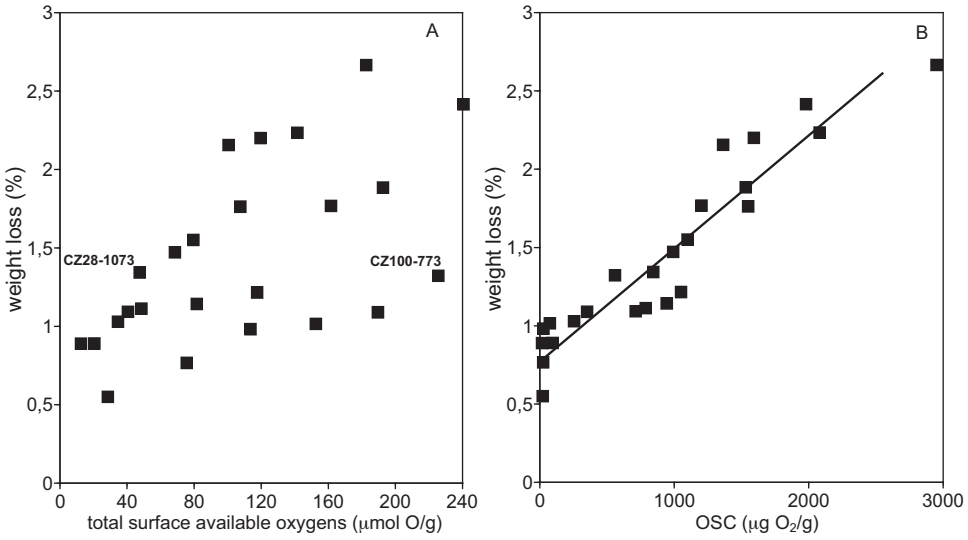

Fig. 8. Weight loss against TSAO (A) and OSC (B) as obtained from TG experiments on soot/catalyst mixtures under inert atmosphere.

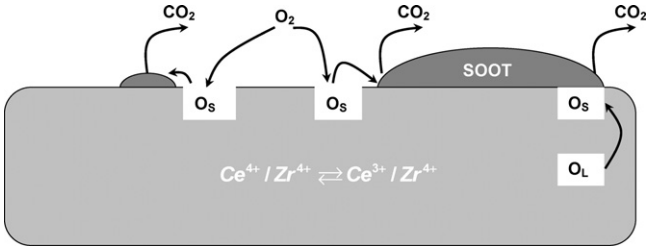

Fig. 9. Schematic representation of oxidation of soot in the presence and absence of gas-phase oxygen.

4. Conclusion

Homogeneous ceria–zirconia solid solutions have been prepared and their structural and textural properties determined by XRD and BET measurements. Thermogravimetric and temperature-programmed methods have been employed to study their soot combustion properties in the presence and absence of oxygen. It is shown that the likely mechanism involves oxidation of soot operated by surface active oxygens donated by ceria–zirconia at a much lower temperature than that possible with gas-phase oxygen. The defect/vacancy created by oxidation is refilled by gaseous oxygen and/or sub-surface bulk oxygen. In the former case the activity is influenced by the amount of surface cerium atoms (which determined the amount of active oxygens) while in the latter case the activity is influenced by OSC of the materials and therefore by composition (Ce/Zr ratio) and only to a lower extent by surface properties. The two mechanisms/phenomena certainly coexist during reaction and their relative significance on the overall reaction is dependent on several factors like accessibility of gaseous oxygen and number, location, shape and dimension of ceria–soot interface.

Acknowledgments

The authors thank financial support from MIUR (progetti PRIN) and regione Friuli Venezia Giulia.

References

[1] W.A. Majewski, M.K. Khair, Diesel Emissions and Their Control, SAE International, Warrendale, PA, USA, 2006.
[2] D. Fino, Sci. Technol. Adv. Mater. 8 (2007) 93–100.
[3] J. Setiabudi, J. Chen, G. Mul, M. Makkee, J.A. Moulijn, Appl. Catal. B 51 (2004) 9–19.
[4] B.A.A.L. van Setten, J.M. Schouten, M. Makkee, J.A. Moulijin, Appl. Catal. B 28 (2000) 253–257.
[5] G. Saracco, C. Badini, N. Russo, V. Specchia, Appl. Catal. B 21 (1999) 233–242.
[6] P. Ciambelli, V. Palma, P. Russo, S. Vaccaro, J. Mol. Catal. A: Chem. 204–205 (2003) 673–681.
[7] B.A.A.L. van Setten, M. Makkee, J.A. Moulijn, Catal. Rev. Sci. Eng. 43 (2001) 489–564.
[8] M.L. Pisarello, V. Milt, M.A. Peralta, C.A. Querini, E.E. Mirò, Catal. Today 75 (2002) 465–470.
[9] A. Carrascull, C. Grzona, D. Lick, M. Ponzi, E. Ponzi, React. Kinet. Catal. Lett. 75 (2002) 63–68.
[10] E.E. Mirò, F. Ravelli, M.A. Ulla, L.M. Cornaglia, C.A. Querini, Catal. Today 53 (1999) 631–638.
[11] V.G. Milt, C.A. Querini, E.E. Miro', M.A. Ulla, J. Catal. 220 (2003) 424–432.
[12] E. Saab, E. Abi-Aad, M.N. Bokova, E.A. Zhilinskaya, A. Aboukaïs, Carbon 45 (2007) 561–567.
[13] S.B. Simonsen, S. Dahl, E. Johnson, S. Helveg, J. Catal. 255 (2008) 1–5.
[14] I. Atribak, A. Bueno-López, A. García-García, Catal. Commun. 9 (2008) 250–255.
[15] M. Issa, C. Petit, A. Brillard, J.-F. Brilhac, Fuel 87 (2008) 740–750.
[16] L. Katta, P. Sudarsanam, G. Thrimurthulu, B.M. Reddy, Appl. Catal. B 101 (2010) 101–108.
[17] K. Shimizu, H. Kawachi, A. Satsuma, Appl. Catal. B 96 (2010) 169–175.
[18] V.G. Milt, M.A. Peralta, M.A. Ulla, E.E. Mirò, Catal. Commun. 8 (2007) 765–769.
[19] J. Liu, Z. Zhao, J. Wang, C. Xu, A. Duan, G. Jiang, Q. Yang, Appl. Catal. B 84 (2008) 185–195.
[20] D. Weng, J. Li, X. Wu, F. Lin, Catal. Commun. 9 (2008) 1898–1901.
[21] Atribak, B. Azambre, A. Bueno-Lopez, A. Garcia-Garcia, Appl. Catal. B 92 (2009) 126–137.
[22] X. Wu, F. Lin, D. Weng, J. Li, Catal. Commun. 9 (2008) 2428–2432.
[23] I. Atribak, A. Bueno-López, A. Garcia-Garcia, Combust. Flame 157 (2010) 2086–2094.
[24] M. Makkee, S.J. Jelles, J.A. Moulijin, in: A. Trovarelli (Ed.), Catalysis by Ceria and Related Materials, Imperial College Press, 2002, p. 391.
[25] E. Aneggi, M. Boaro, C. de Leitenburg, G. Dolcetti, A. Trovarelli, Catal. Today 112 (2006) 94–98.
[26] E. Aneggi, M. Boaro, C. de Leitenburg, G. Dolcetti, A. Trovarelli, J. Alloys Compd. 408–412 (2006) 1096–1102.
[27] E. Aneggi, C. de Leitenburg, G. Dolcetti, A. Trovarelli, Catal. Today 114 (2006) 40–47.
[28] E. Aneggi, C. de Leitenburg, G. Dolcetti, A. Trovarelli, Top. Catal. 42–43 (2007) 319–322.
[29] E. Aneggi, C. de Leitenburg, G. Dolcetti, A. Trovarelli, Catal. Today 136 (2008) 3–10.
[30] A. Bueno-Lopez, K. Krishna, M. Makkee, J.A. Moulijin, J. Catal. 230 (2005) 237–248.
[31] K. Krishna, A. Bueno-Lopez, M. Makkee, J.A. Moulijn, Appl. Catal. B 75 (2007) 189–200.
[32] K. Krishna, A. Bueno-Lopez, M. Makkee, J.A. Moulijn, Appl. Catal. B 75 (2007) 201–209.
[33] K. Krishna, A. Bueno-Lopez, M. Makkee, J.A. Moulijn, Appl. Catal. B 75 (2007) 210–220.
[34] L. Zhu, J. Yu, X. Wang, J. Hazard. Mater. 140 (2007) 205–210.
[35] M.A. Peralta, V.G. Milt, L.M. Cornaglia, C.A. Querini, J. Catal. 242 (2006) 118–130.
[36] X. Wu, D. Liu, K. Li, J. Li, D. Weng, Catal. Commun. 8 (2007) 1274–1278.

[37] B. Bassou, N. Guilhaume, K. Lombaert, C. Mirodatos, D. Bianchi, Energy Fuels 24 (2010) 4766–4780.
[38] B. Bassou, N. Guilhaume, K. Lombaert, C. Mirodatos, D. Bianchi, Energy Fuels 24 (2010) 4781–4792.
[39] A. Trovarelli, Comments Inorg. Chem. 20 (1999) 263–284.
[40] R. Di Monte, J. Kaspar, Catal. Today 100 (2005) 27–35.
[41] Q. Liang, X. Wu, X. Wu, D. Weng, Catal. Lett. 119 (2007) 265–270.
[42] A. Bueno-López, K. Krishna, M. Makkee, J.A. Moulijn, Catal. Lett. 99 (2005) 203–205.
[43] A. Pappacena, K. Schermanz, A. Sagar, E. Aneggi, A. Trovarelli, Stud. Surf. Sci. Catal. 175 (2010) 835–838.
[44] R. Jenkins, R. Snyder, Introduction to X-ray Powder Diffractometry, Wiley, New York, 1996, p. 90.
[45] R.A. Young, The Rietveld Method, IUCr Oxford University Press, New York, 1993.
[46] A.C. Larson, R.B. Von Dreele, General Structure Analysis System (GSAS), Los Alamos National Laboratory Report LAUR 86-748, 2000.
[47] B.H. Toby, J. Appl. Crystallogr. 34 (2001) 210–213.
[48] J.P.A. Neeft, M. Makkee, J.A. Moulijn, Chem. Eng. J. 64 (1996) 295–302.
[49] J.P.A. Neeft, O.P. van Pruissen, M. Makkee, J.A. Moulijn, Appl. Catal. B 12 (1997) 21–31.
[50] G.A. Stratakis, A.M. Stamatelos, Combust. Flame 132 (2003) 157–159.
[51] J.P.A. Neeft, M. Makkee, J.A. Moulijn, Appl. Catal. B 8 (1996) 57–78.
[52] G. Neri, G. Rizzo, S. Galvagno, M.G. Musolino, A. Donato, R. Pietropaolo, Thermochim. Acta 381 (2002) 165–172.
[53] J.F. Lamonier, N. Sergent, J. Matta, A. Aboukaïs, J. Therm. Anal. Calorim. 66 (2001) 645–658.
[54] B.R. Stanmore, J.F. Brilhac, P. Gilot, Carbon 39 (2001) 2247–2268.
[55] S.J. Jelles, B.A.A.L. Van Setten, M. Makkee, J.A. Moulijn, Appl. Catal. B 21 (1999) 35–49.
[56] G. Mul, F. Kapteijn, J.A. Moulijn, Appl. Catal. B 12 (1997) 33–47.
[57] Z. Sarbak, K. Surma, J. Therm. Anal. Calorim. 72 (2003) 159–163.
[58] E. Mamontov, R. Brezny, M. Koranne, T. Egami, J. Phys. Chem. B 107 (2003) 13007–13014.
[59] V. Perrichon, A. Laachir, S. Abouarnadasse, O. Touret, G. Blanchard, Appl. Catal. A 129 (1995) 69–82.
[60] J. Kaspar, P. Fornasiero, in: A. Trovarelli (Ed.), Catalysis by Ceria and Related Materials, Imperial College Press, London, 2002, pp. 217–241.
[61] S. Rossignol, Y. Madier, D. Duprez, Catal. Today 50 (1999) 261–270.
[62] A. Trovarelli, M. Boaro, E. Rocchini, C. de Leitenburg, G. Dolcetti, J. Alloys Compd. 323–324 (2001) 584–591.
[63] P. Fornasiero, G. Balducci, R. Di Monte, J. Kašpar, V. Sergo, G. Gubitosa, A. Ferrero, M. Graziani, J. Catal. 164 (1996) 173–183.
[64] V. Sanchez Escribano, E. Fernandez Lopez, M. Panizza, C. Resini, J.M. Gallardo Amores, G. Busca, Solid State Sci. 5 (2003) 1369–1376.
[65] H. Vidal, J. Kaspar, M. Pijolat, G. Colon, S. Bernal, A. Cordon, V. Perrichon, F. Fally, Appl. Catal. B 30 (2001) 75–85.
[66] J. Kaspar, P. Fornasiero, M. Graziani, Catal. Today 50 (1999) 285–298.
[67] J. van Doorn, J. Varloud, P. Meriaudeau, V. Perrichon, Appl. Catal. B 1 (1992) 117–127.
[68] P. Palmisano, N. Russo, P. Fino, D. Fino, C. Badini, Appl. Catal. B 69 (2006) 85–92.
[69] K. Krishna, A. Bueno-López, M. Makkee, J.A. Moulijn, Top. Catal. 42–43 (2007) 221–228.
[70] P. Fang, M. Luo, J. Lu, S. Cen, X. Yan, X. Wang, Thermochim. Acta 478 (2008) 45–50.
[71] M.A. Malecka, L. Kepinski, W. Mista, Appl. Catal. B 74 (2007) 290–298.
[72] A. Trovarelli, Catal. Rev. Sci. Eng. 38 (1996) 439–520.
[73] Y. Madier, C. Descorme, A.M. LeGovic, D. Duprez, J. Phys. Chem. B 103 (1999) 10999–11006.
[74] C.E. Hori, H. Permana, K.Y. Simon Ng, A. Brenner, K. More, K.M. Rhamoeller, D. Belton, Appl. Catal. B 16 (1998) 105–117.
[75] M. Boaro, C. de Leitenburg, G. Dolcetti, A. Trovarelli, J. Catal. 193 (2000) 338–347.
[76] A. Trovarelli, F. Zamar, J. Lorca, C. de Leitenburg, G. Dolcetti, J.T. Kiss, J. Catal. 169 (1997) 490–502.